PLOS ONE

RESEARCH ARTICLE

M30 Antagonizes Indoleamine 2,3-Dioxygenase Activation and Neurodegeneration Induced by Corticosterone in the Hippocampus

Chun-Sing Lam[1], George Lim Tipoe[1,2], Johnny Kong-Ching Wong[3], Moussa B. H. Youdim[4], Man-Lung Fung[1,2]*

1 School of Biomedical Sciences, The University of Hong Kong, Hong Kong, Hong Kong SAR, **2** Research Centre of Heart, Brain, Hormone & Healthy Aging, Li Ka Shing Faculty of Medicine, The University of Hong Kong, Hong Kong, Hong Kong SAR, **3** Department of Pharmacology & Pharmacy, The University of Hong Kong, Hong Kong, Hong Kong SAR, **4** Eve Topf Center for Neurodegenerative Diseases Research, Faculty of Medicine, Technion-Israel Institute of Technology, Haifa, 31096, Israel

* fungml@hku.hk

OPEN ACCESS

Citation: Lam C-S, Tipoe GL, Wong JK-C, Youdim MBH, Fung M-L (2016) M30 Antagonizes Indoleamine 2,3-Dioxygenase Activation and Neurodegeneration Induced by Corticosterone in the Hippocampus. PLoS ONE 11(11): e0166966. doi:10.1371/journal.pone.0166966

Editor: Kenji Hashimoto, Chiba Daigaku, JAPAN

Received: August 9, 2016

Accepted: November 6, 2016

Published: November 21, 2016

Data Availability Statement: All relevant data are within the paper and its Supporting Information files.

Funding: This study was supported by the University of Hong Kong, grant number: 104003406, www.hku.hk.

Competing Interests: The authors have declared that no competing interests exist.

Abstract

Monoamine oxidases (MAO), downstream targets of glucocorticoid, maintain the turnover and homeostasis of monoamine neurotransmitters; yet, its pathophysiological role in monoamine deficiency, oxidative stress and neuroinflammation remains controversial. Protective effects of M30, a brain selective MAO inhibitor with iron-chelating antioxidant properties, have been shown in models of neurodegenerative diseases. This study aims to examine the neuroprotective mechanism of M30 against depressive-like behavior induced by corticosterone (CORT). Sprague-Dawley rats were given CORT subcutaneous injections with or without concomitant M30 administration for two weeks. CORT-treated rats exhibited depressive-like behavior with significant elevated levels of MAO activities, serotonin turnover, oxidative stress, neuroinflammation and apoptosis in the hippocampus with significant losses of synaptic proteins when compared to the control. The expression and activity of cytokine-responsive indoleamine 2,3-dioxygenase (IDO-1), a catabolic enzyme of serotonin and tryptophan, was significantly increased in the CORT-treated group with lowered levels of serotonin. Besides, CORT markedly reduced dendritic length and spine density. Remarkably, M30 administration neutralized the aberrant changes in the hippocampus and prevented the induction of depressive-like behavior induced by CORT. Our results suggest that M30 is neuroprotective against CORT-induced depression targeting elevated MAO activities that cause oxidative stress and neuroinflammation, resulting in IDO-1 activation, serotonin deficiency and neurodegeneration.

Introduction

Major depressive disorder is a life-threatening psychological disorder highly prevalent in the worldwide population [1, 2]. Clinically, depression is closely associated with hypercortisolemia in patients, which may be involved in the atrophy and dysfunction of the hippocampus [3, 4]. This is consistent with the findings that chronic exposure to corticosterone (CORT) induces depressive-like behavior in rodents with aberrant dendritic arborization and impaired synaptic plasticity in the hippocampus [5, 6]; yet the pathophysiological mechanism of chronic CORT treatment leading to the monoamine deficiency and neurodegeneration remains controversial.

Monoamine oxidases (MAO), with two isoforms A and B, are enzymes located at the outer membrane of mitochondria that catalyze the oxidative deamination of monoamine neurotransmitters and produce hydrogen peroxide as a by-product [7]. MAO-A is mainly responsible for the deamination of serotonin, norepinphrine and dopamine, whereas MAO-B degrades phenethylamine, benzylamine and dopamine [8]. Elevated brain MAO-A activities have been reported in both living and post-mortem tissues of clinically depressed patients [9–11], which were also found to be implicative in the pathogenesis of stress-induced depressive-like behaviors in experimental animals [12, 13]. Anomalous activation of the MAO-A activity could alter the turnover and availability of monoamines resulting in serotonin deficiency, manifested as one of the major clinical observations [14]. Thus, pharmacological inhibition of MAO-A is a first-line clinical treatment for the patient [15]. Notably, MAO-A is one of the main downstream targets of glucocorticoids and potentially plays a pathophysiological role in CORT-induced depressive-like behavior. However, the mechanistic effect of blockade of MAO activities against the pathophysiological cascade of CORT-induced depressive-like behavior remains unclear. In this context, recent studies proposed a significant role of neuroinflammation in the brain of clinically depressed patients [16]. Putatively, it could induce depressive-like behavior in rodents with an activation of inflammatory cytokines-responsive indoleamine 2,3-dioxygenase (IDO-1), which is a key enzyme for the catabolism of tryptophan and serotonin, that could deplete the level of serotonin [17, 18]. In addition, the metabolites of IDO-1 have been reportedly shown to induce neuronal apoptosis and neurodegeneration as a result of IDO-1 activation [19, 20]. Yet, it remains elusive the role of neuroinflammation and IDO-1 in CORT-induced depression.

M30, 5(-N-Methyl-N-propargylaminomethyl)-8- hydroxyquinoline), is brain-permeable to the blood brain barrier and is a potent brain-selective MAO inhibitor with chemical properties of iron-chelating free radical scavengers [21]. It is composed of propargyl moiety for the MAO inhibition and the prototype of iron-chelator VK28. Experimental studies have demonstrated the beneficial effect of M30 against the pathogenic cascade of neurodegenerative processes in rodent models of Alzheimer's or Parkinson disease, via suppressing the brain MAO activity and oxidative stress [22, 23]. Recently, M30 has also been shown to effectively alleviate the elevated level of inflammatory cytokines in a mouse model of Alzheimer's disease [24]. However, the mechanistic effect of M30 against neuroinflammation induced by CORT remains elusive. We hypothesized that M30 is neuroprotective against CORT-induced depressive-like behavior. This study focused on the pathophysiological mechanism leading to the CORT-induced depressive-like behavior, in which oxidative stress and neuroinflammation mediated by over-activation of MAO and IDO-1 activities could significantly contribute to the serotonin deficiency and neurodegeneration.

Materials and Methods

Animals and experimental grouping

All experimental procedures were approved and conducted according to the Committee on the Use of Live Animals in Teaching and Research (CULATR #2522–11, 3545–15), The

University of Hong Kong. The Laboratory Animal Unit of the University of Hong Kong is fully accredited by the Association for Assessment and Accreditation of Laboratory Animal Care International (AAALAC international). Adult male Sprague Dawley rats (220–250 g) were put under pathogen-free condition in an air-conditioned room at constant temperature (23±1˚C) provided with water and standard diet (LabDiet, 5053 (LabDiet; St. Louis, MO, USA)) ad libitum. All animals were monitored on a daily basis for body health throughout the study. There were five experimental groups (n = 12 per group), namely non-treated control (Control), M30-treated groups (M30), corticosterone-treated group (CORT), corticosterone and M30 co-treated group (CORT + M30) and vehicle-treated group (Vehicle).

Drug preparation and treatment

Drug M30, 5(-N-Methyl-N-propargylaminomethyl)-8- hydroxyquinoline) was kindly provided by Dr. Moussa Youdim and Dr. Lin Bin. M30 solution was freshly prepared by dissolving in saline. Corticosterone (Sigma, St Louis) was prepared daily using sesame oil as vehicle and injected subcutaneously (near the cervical region) according to the method described by Hellsten et al. [25]. A daily injection of corticosterone at a dose of 50 mg/kg for consecutive 14 days significantly elevated the levels of CORT (S1 Table) and MAO expression (S1 Fig) and also induced depressive-like behavior in rats as previously reported [6]. M30 at a dose of 5 mg/kg was intraperitoneally injected to the animals with or without CORT co- treatment for 14 days. The animals were anesthetized with halothane and then decapitated to harvest the hippocampus for experiments.

Measurement of MAO-A and MAO-B activities

Hippocampi were homogenized in 50 mM potassium phosphate buffer (pH = 7.4) and the lysate was diluted in the reaction buffer provided by Amplex Red Monoamine Oxidase Assay Kit (Invitrogen, CA, USA). The MAO-A enzyme activity was quantified according to the manufacture protocol and was normalized to total protein content in each sample. The results were expressed as percentage of the control.

Western Blot

Protein expressions of hippocampal tissue lysate (including cytosolic and nuclear fractions) were performed as previously described [26]. The expression of β-actin served as the internal control for whole cell lysate and cytosolic fraction protein, whereas Lamin B1 served as the internal control of nuclear fraction protein. Primary antibodies of SOD-2 (rabbit polyclonal, 1:1000), GPx-1 (goat polyclonal, 1:500), NFκB p65 (rabbit polyclonal, 1:250) and p50 (mouse monoclonal, 1:250), IκBα (mouse monoclonal, 1:500), TNF α (goat polyclonal, 1:80), IL-1β (rabbit polyclonal 1:100), IL-6 (goat polyclonal, 1:1000) and COX-2 (goat polyclonal, 1:100) were purchased from Santa Cruz Biotechnology, CA, USA; Synapsin 1 (rabbit polyclonal, 1:500) and Synaptophysin (rabbit polyclonal, 1:2000) were purchased from Novus Biologicals, USA; PSD95 (rabbit polyclonal 1:500), Cleaved Caspase 3 (rabbit polyclonal 1:500) was purchased from Cell Signaling Technology; Cleaved PARP-1 (rabbit polyclonal, 1:2000) was purchased from Bioworld Technology; IDO-1 (rabbit polyclonal, 1:250) was purchased from antibodies-online (ABIN1714836). The optical density of the bands was measured and quantified by Image J (National Institute of Health, MD, USA). The data were expressed as percentage of the control.

Enzyme-Linked Immunosorbent Assay (ELISA)

According to manufacturers' protocol, ELISA kits were employed to measure the levels of serotonin (5-HT) (Enzo Life Sciences), 5-HT metabolite (5-HIAA) (Elabscience), tryptophan

(TRP) (LDN Labor Diagnostika Nord GmbH & Co.KG), Kynurenine (KYN) (MyBioSource) and Quinolinic acid (QUIN) (Cloud-Clone Corp.) in the hippocampal tissue lysate. The results were expressed as ng/gram wet tissue and nM respectively.

Malondialdehyde (MDA) Assay

MDA amount of hippocampal samples was measured by Bioxytech LPO-586TM kit (OxisResearch, Portland, OR). In brief, according to manufacturer's instruction, the reaction products were read at 586 nm followed by normalization of corresponding protein amount measured by Bio-Rad Protein Assay Kit (Bio-Rad, Hercules, CA). Standard curve was constructed with 1,1,3,3-tetraethoxypropan. The results were expressed as μmol/mg and percentage of the control.

GSH/GSSG Ratio

Hippocampus was homogenized with 5% metaphosphoric acid followed by centrifugation at 14,000g for 15min at 4˚C to obtain the supernatant. According to manufacturer's protocol, the total amount of glutathione (GSH) and oxidized glutathione (GSSG) were determined. The amount of reduced GSH was calculated using the equation: Reduced GSH = Total glutathione–oxidized GSSG. The results were expressed as GSH/GSSG ratio.

Golgi Staining

Golgi staining was performed to reveal morphological features of hippocampal neurons with the use of FD Rapid GolgistainTM Kit (FD Neurotechnologies, MD). According to the manufacturer's instruction, hippocampal CA1 and CA3 pyramidal neurons are visualized for the analysis of dendritic length and spine density. Five neurons from each 100μm-thick transverse section of the hippocampus were sampled and analyzed with the use of Neurolucida software (MicroBright-Field, USA). Neurons selected for the analysis were relatively isolated and distinguished from neighboring impregnated neurons to avoid interference. The area of cell bodies, dendritic length and spine density of both apical and basal branches were quantified. The volume of cell body was calculated with the use of the mathematic equation: $4/3\pi r^3$. For the dendritic length and spine density, a minimum of three to five with at least one branch point were selected for counting. Visible spines along the branch segment were counted and the spine density was expressed as number per 10μm.

Behavioral Tests

Forced swimming test (FST) was employed to examine the depressive-like behavior of the rats. The immobility time served as the valid indicator of behavioral despair according to the previous reports [27, 28]. In brief, rats were placed in a cylinder (60cm height X 25 cm diameter) containing tap water for 15-min training session to learn helplessness on the first day after 2-week CORT treatment. Rats were then put into the water again for 5 minutes and the performance was recorded on the second day. The immobility time was evaluated.

Reward-based sucrose consumption was carried out to assess the hedonic status of the rodents with the use of sucrose preference test (SPT) [29, 30]. Another independent batch of rats were individually caged and given the training session in which two bottles of 1% (wt/vol) sucrose solution for 24 hours on the first day after 2-week CORT treatment to prevent the subtle stress when applying the sucrose consumption assessment. After that, the rats were

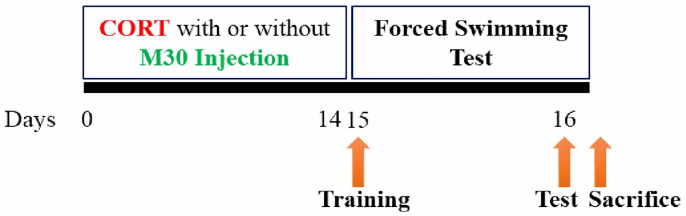
CORT with or without
M30 Injection
Forced Swimming
Test
Days 0
14 15
16
Training
Test Sacrifice

A

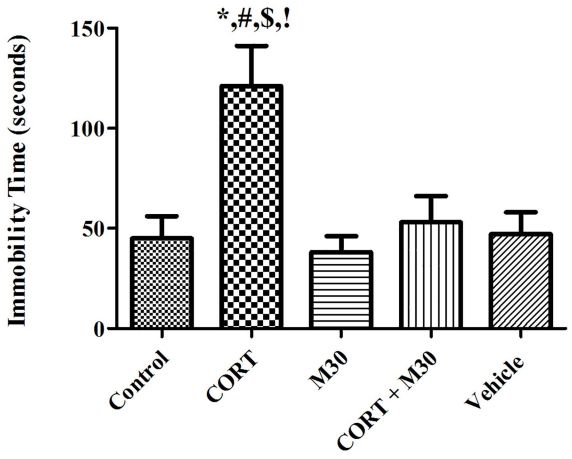
*,#,$,!
Immobility Time (seconds)
150
100
50
0
Control
CORT
M30
CORT + M30
Vehicle

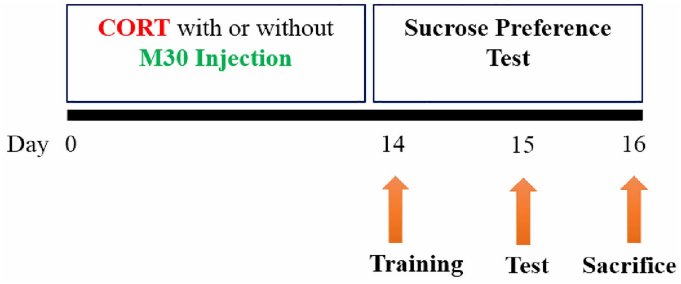
CORT with or without
M30 Injection
Sucrose Preference
Test
Day 0
14
15
16
Training
Test
Sacrifice

B

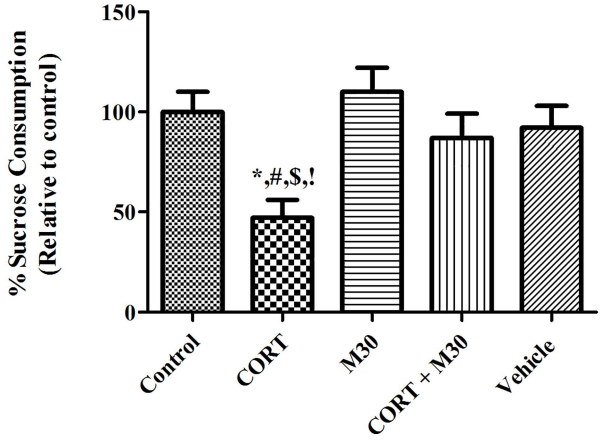
% Sucrose Consumption
(Relative to control)
150
100
50
0
*,#,$,!
Control
CORT
M30
CORT + M30
Vehicle

Fig 1. Chronic CORT treatment induced depressive-like behavior in rats, which was significantly ameliorated by the M30 administration. Panels A and B summarize the immobility time and percentage of sucrose consumption of the animals in the control, CORT-treated (CORT), M30-treated (M30), CORT and M30 co-treated (CORT+M30) or vehicle groups respectively. Data from each group were expressed as mean ± SEM (n = 12). Statistical comparisons between groups were performed using the One way Anova followed by Tukey post hoc test to detect differences in all groups. For FST, *p < 0.001 when compared with Control, $^{\#}$p < 0.001 when compared with M30, $^{\$}$p < 0.001 when compared with CORT + M30 groups,$^{!}$ p < 0.001 when compared with Vehicle. For SPT, *p < 0.01 when compared with Control, $^{\#}$p < 0.01 when compared with M30, $^{\$}$p < 0.01 when compared with CORT + M30 groups,$^{!}$ p < 0.05 when compared with Vehicle.

doi:10.1371/journal.pone.0166966.g001

provided one bottle of water and the other contained 1% (wt/vol) sucrose solution for 24 hours. The positions of bottles were swapped in the middle of the assessment to avoid the bias towards a particular side. No food and water deprivation was applied before the test to prevent the interference with the metabolic demands of the rats. The consumption of water and sucrose solution was recorded by weighing bottles before and after the test. Sucrose consumption was presented as the percentage of the sucrose solution over the total weight of liquid consumed. The data were expressed as percentage of the control.

Statistical Analysis

Data from each group were expressed as mean ± SEM. Statistical comparisons among groups were performed using One way ANOVA followed by Tukey's post-hoc test for multiple comparisons. A $p<0.05$ was considered to be statistically significant with the use of Graphpad Prism® software (Graphpad Software Version 5.01, Inc., San Diego, USA)

Results

M30 antagonized CORT-induced depressive-like behaviors

The immobility time in the forced swimming test and the percentage of sucrose consumption in the sucrose preference test were, respectively, increased and reduced significantly in the CORT-treated group when compared to the control and vehicle groups ($p<0.001$ for FST, $p<0.01$ for SPT) (n = 12, Fig 1). There were no differences between the control and the M30-treated groups with or without the CORT treatment (Fig 1). Results indicated that chronic CORT treatment induced depressive-like behavior in the rat, which was significantly prevented by the M30 administration.

M30 mitigated CORT-induced MAO over-activation

The activity of MAO-A was doubled in the CORT-treated group when compared with that of the control group ($p<0.001$) (n = 8), but was significantly prevented by the M30 treatment (Fig 2). Besides, there was a significant decrease in the MAO-A activity by 50% in the M30-treated group, when compared with that of the control or vehicle group ($p<0.01$) (Fig 2). The level of 5-HT was significantly reduced by 40% in the CORT-treated group when compared with that of the control group ($p<0.001$) (n = 8). The level of 5-HIAA was significantly elevated by 50% in the CORT-treated group when compared with that of the control group ($p<0.001$) (n = 8). In addition, the ratio of 5-HIAA/5-HT was significantly increased in the CORT-treated group when compared with the control ($p<0.001$). However, there was no significant change in the levels of 5-HT and 5-HIAA in the M30-treated group.

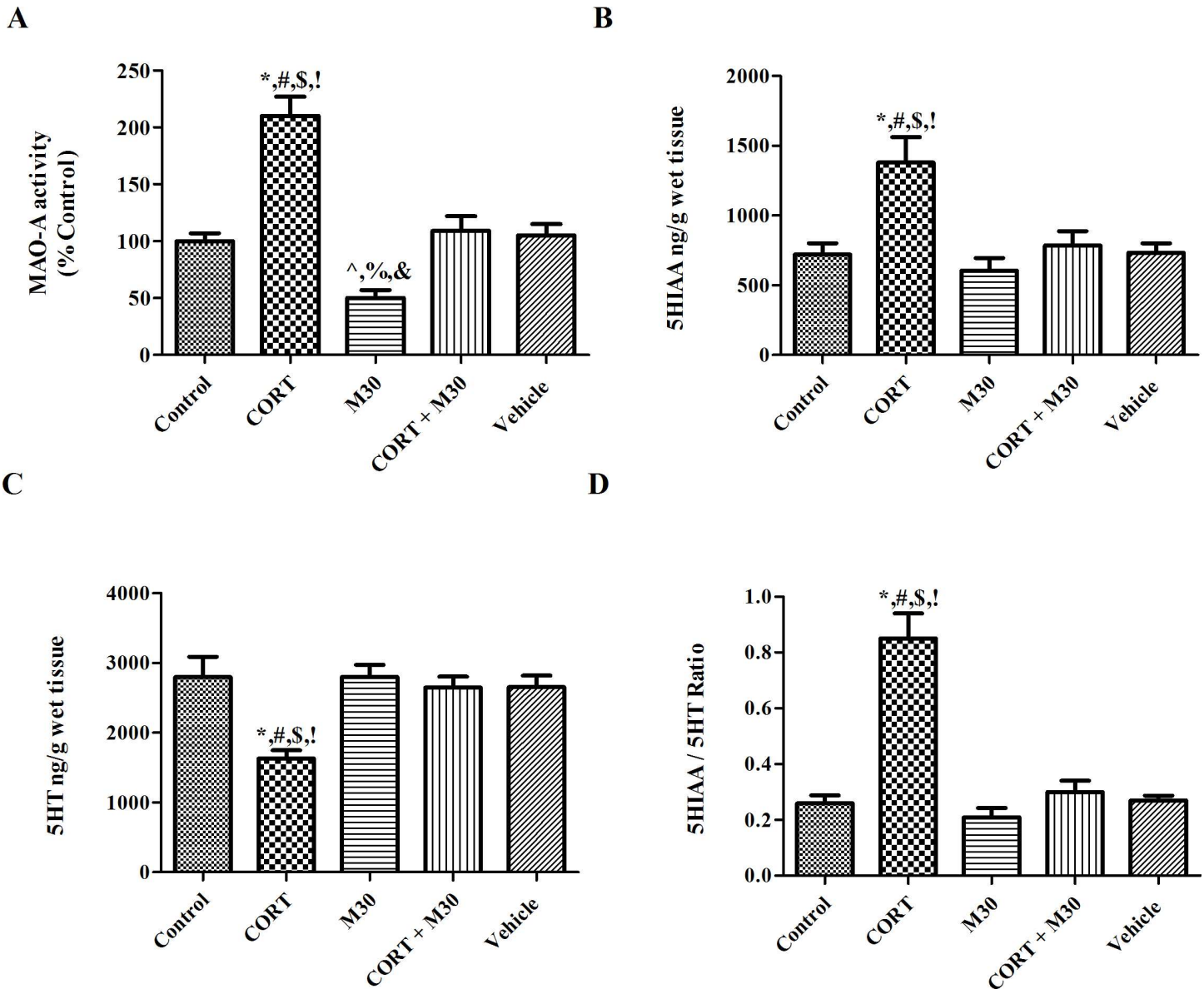

Fig 2. MAO-A activity and serotonin (5HT) turnover were increased in the hippocampus of CORT-treated group, which was significantly attenuated by M30. Figures A-D summarize the levels of (A) MAO-A activity, (B) 5HIAA, (C) 5HT and (D) the ratio of 5HIAA/5HT in the hippocampus of the control, CORT-treated (CORT), M30-treated (M30), CORT and M30 co-treated (CORT+M30) or vehicle groups. β-actin was the internal control. Data from each group were expressed as mean ± SEM (n = 8). Statistical comparisons between groups were performed using the One way Anova followed by Tukey post hoc test to detect differences in all groups. For MAO-A activity, *$p < 0.001$ when compared with Control, $^{\#}p < 0.001$ when compared with M30, $^{\$}p < 0.001$ when compared with CORT + M30 groups,$^{!}$ $p < 0.001$ when compared with Vehicle, $^{\wedge}p < 0.01$ when compared with Control, $^{\%}p < 0.01$ when compared with CORT + M30, $^{\&}p < 0.01$ when compared with Vehicle groups. For 5HIAA, 5HT and 5HIAA/5HT ratio, *$p < 0.001$ when compared with Control, $^{\#}p < 0.001$ when compared with M30, $^{\$}p < 0.001$ when compared with CORT + M30 groups,$^{!}$ $p < 0.001$ when compared with Vehicle.

doi:10.1371/journal.pone.0166966.g002

M30 attenuated CORT-induced oxidative stress

The MDA level in the hippocampus was markedly elevated by 2 folds in the CORT-treated group when compared with that of the control group ($p<0.001$) (n = 8, Fig 3). The increased MDA level was significantly attenuated in the group co-treated with M30 (Fig 3). Additionally, levels of the GSH/GSSH ratio ($p<0.01$) and protein expressions of antioxidant enzymes GPx-1

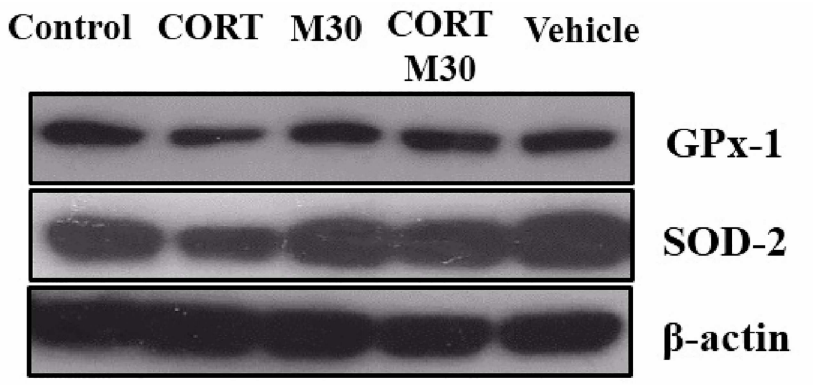
Control
CORT
M30
CORT M30
Vehicle
GPx-1
SOD-2
β-actin

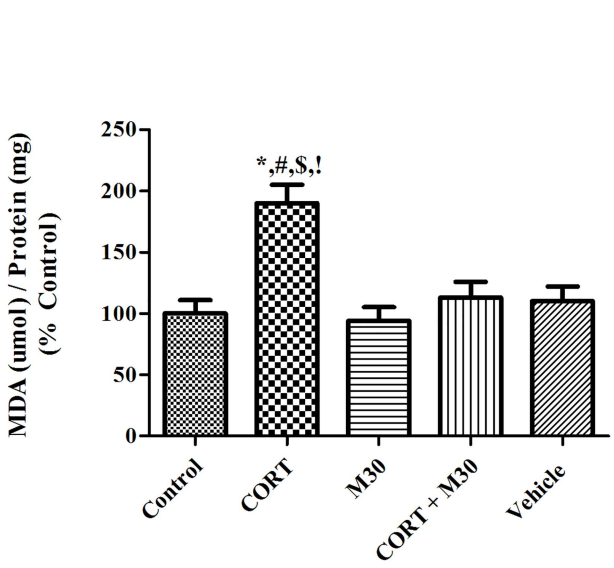
A
MDA (umol) / Protein (mg) (% Control)
250
200
150
100
50
0
*,#,$,!
Control
CORT
M30
CORT + M30
Vehicle

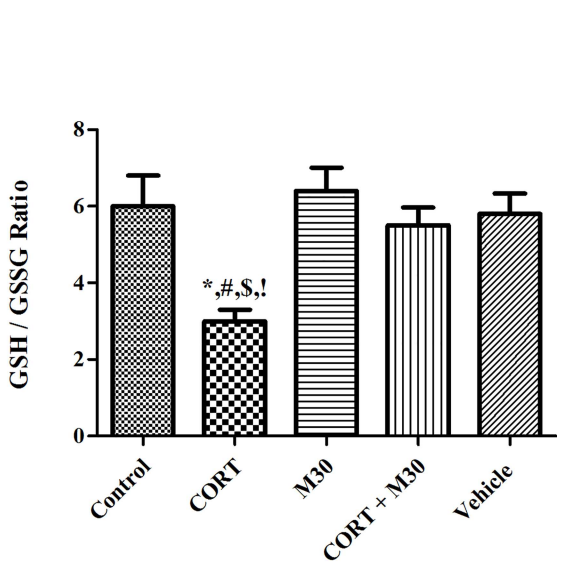
B
GSH / GSSG Ratio
8
6
4
2
0
*,#,$,!
Control
CORT
M30
CORT + M30
Vehicle

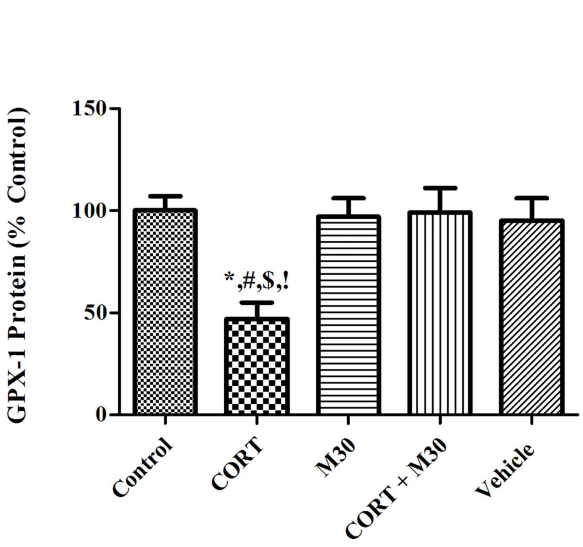
C
GPX-1 Protein (% Control)
150
100
50
0
*,#,$,!
Control
CORT
M30
CORT + M30
Vehicle

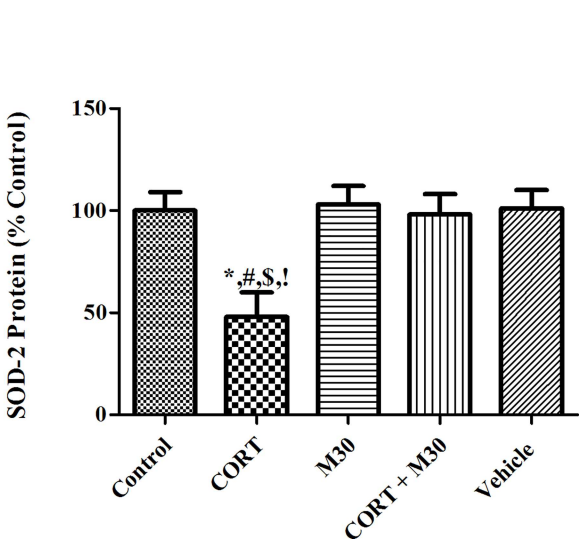
D
SOD-2 Protein (% Control)
150
100
50
0
*,#,$,!
Control
CORT
M30
CORT + M30
Vehicle

Fig 3. M30 attenuated MAO-induced oxidative stress. Levels of (A) MDA content, (B) GSH/GSSG ratio, and the protein expression of (C) GPx-1 and (D) SOD-2 in the hippocampus of the control, CORT-treated (CORT), M30-treated (M30), CORT and M30 co-treated (CORT+M30) or vehicle groups are summarized in the figures. β-actin was an internal control. Data from each group were expressed as mean ± SEM (n = 8). Statistical comparisons between groups were performed using the One way Anova followed by Tukey post hoc test to detect differences in all groups. For MDA, *p < 0.001 when compared with Control, $^{\#}$p < 0.001 when compared with M30, $^{\$}$p < 0.01 when compared with CORT + M30 groups,$^{!}$ p < 0.001 when compared with Vehicle. For GSH/GSSG ratio, GPx-1 and SOD-2, *p < 0.01 when compared with Control, $^{\#}$p < 0.01 when compared with M30, $^{\$}$p < 0.05 when compared with CORT + M30 groups,$^{!}$ p < 0.05 when compared with Vehicle.

doi:10.1371/journal.pone.0166966.g003

and SOD-2 ($p<0.01$ for both) in the CORT-treated group were significantly reduced by 50% of the control or vehicle group, which was normalized by the M30 treatment.

M30 suppressed neuroinflammation via redox-sensitive NFKB canonical pathway

The amount of total I-kappa-Bα, the negative regulator of NFKB canonical cascade was significantly decreased in the CORT-treated group when compared with the control groups ($p<0.001$) (n = 8, Fig 4). Consistently, the nuclear-fractional expressions of p65 and p50 were significantly augmented by 3.5 and 2.5 folds ($p<0.001$ for both), respectively, whereas the cytosolic fractional expressions of p65 and p50 were remarkably lowered by 80% and 90%, respectively ($p<0.001$ for both). The degradation of I-kappa-Bα and translocation of NFKB members p65 and p50 were significantly repressed by the M30 treatment (Fig 4). Also, the protein expressions of inflammatory cytokines TNFα, IL-1β, IL-6 and COX-2 were significantly elevated by 2–2.5 folds in the CORT-treated group when compared with that of the control or vehicle group ($p<0.001$ for all) (n = 8). The elevated levels of cytokine were significantly ameliorated by the M30 treatment (Fig 5).

M30 blocked the expression and activity of IDO-1 and attenuated the level of QUIN

The protein expression of IDO-1 in the CORT-treated group was 2.5 folds higher than that of the control or vehicle group (n = 8, Fig 5). The level of TRP was reduced by 30% in the CORT-treated group when compared with that of the control ($p<0.01$) whereas the level of KYN was elevated by 40% in the CORT-treated group when compared with that of the control ($p<0.01$). The kynurenine to tryptophan (KYN/TRP) ratio was doubled in the CORT-treated group when compared with that of the control ($p<0.01$). IDO-1 downstream metabolite quinolinic acid was significantly elevated in the CORT-treated group when compared with that of control ($p<0.01$). The increased levels of IDO-1 expression, TRP, KYN, KYN/TRP ratio and QUIN were significantly attenuated in the group co-treated with M30 (Fig 5).

M30 abrogated CORT-induced hippocampal apoptosis

The expression level of anti-apoptotic protein Bcl-2 in the CORT-treated group was significantly less by half of that of the control group ($p<0.01$). In addition, levels of the apoptotic markers, cleaved-caspase-3 and cleaved-PARP-1, were increased by 3 folds in the CORT-treated group when compared with those of the control or vehicle group ($p<0.001$ for both) (n = 8, Fig 6). No changes were found in the M30-treated groups when comparing to the control (Fig 6).

M30 restored CORT-induced loss of synaptic proteins

There were significant decreases in the pre-synaptic vesicle proteins synapsin-1 and synaptophysin, and post-synaptic protein PSD-95, respectively by 90%, 30% and 50% in the CORT-

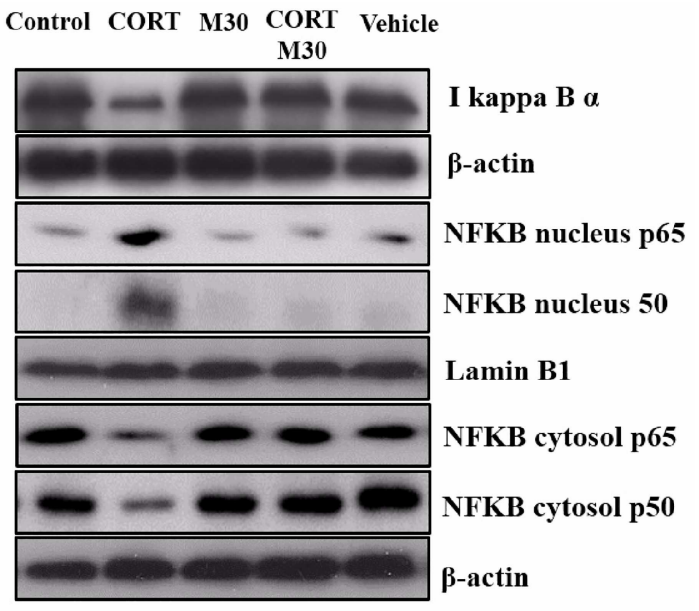
Control
CORT
M30
CORT M30
Vehicle
I kappa B α
β-actin
NFKB nucleus p65
NFKB nucleus 50
Lamin B1
NFKB cytosol p65
NFKB cytosol p50
β-actin

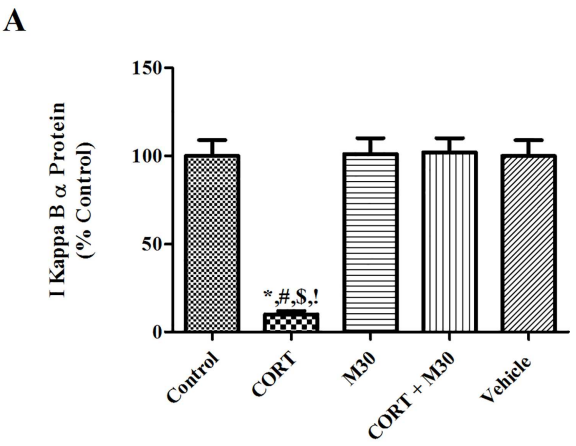
A
I Kappa B α Protein (% Control)
150
100
50
0
*,#,$,!
Control
CORT
M30
CORT + M30
Vehicle

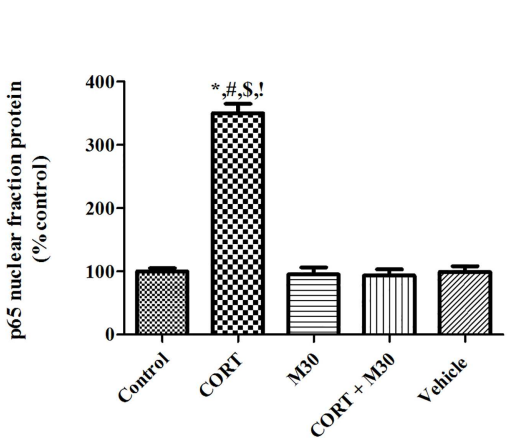
B
p65 nuclear fraction protein (% control)
400
300
200
100
0
*,#,$,!
Control
CORT
M30
CORT + M30
Vehicle

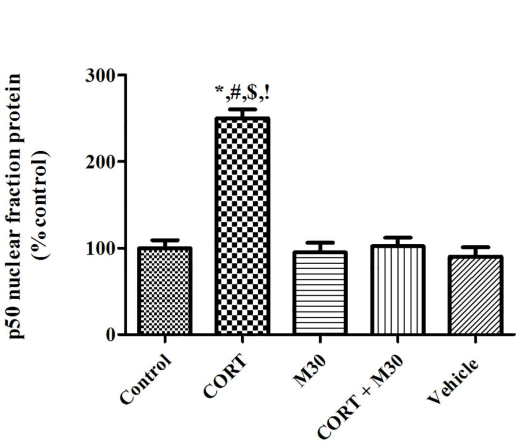
C
p50 nuclear fraction protein (% control)
300
200
100
0
*,#,$,!
Control
CORT
M30
CORT + M30
Vehicle

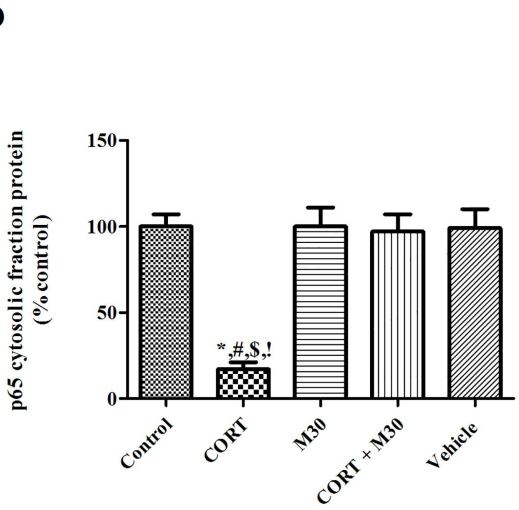
D
p65 cytosolic fraction protein (% control)
150
100
50
0
*,#,$,!
Control
CORT
M30
CORT + M30
Vehicle

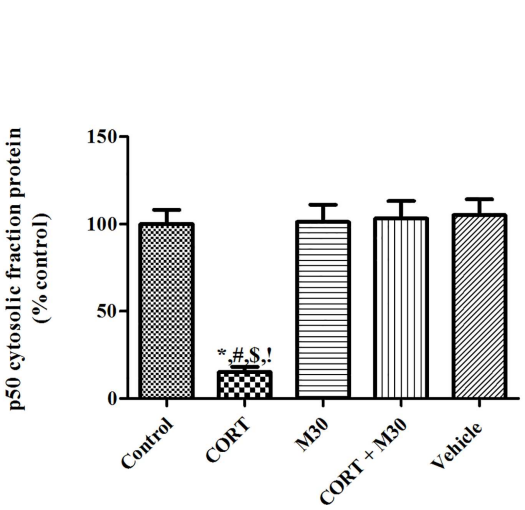
E
p50 cytosolic fraction protein (% control)
150
100
50
0
*,#,$,!
Control
CORT
M30
CORT + M30
Vehicle

Fig 4. M30 prevented the degradation of redox-sensitive NFKB canonical pathway negative regulator IKBα and repressed the nucleus translocation of NFKB member p65 and p50 from cytosol. Levels of protein expression of (A) IKB α, nuclear protein expression of (B) p65 and (C) p50, and cytosolic protein expressions of (D) p65 and (E) p50 in the hippocampus of the control, CORT-treated (CORT), M30-treated (M30), CORT and M30 co-treated (CORT+M30) or vehicle groups are summarized. Lamin B1 and β-actin were an internal control of the nuclear fraction cytosolic fraction respectively. Data from each group were expressed as mean ± SEM (n = 8). Statistical comparisons between groups were performed using the One way Anova followed by Tukey post hoc test to detect differences in all groups. *$p < 0.001$ when compared with Control, #$p < 0.001$ when compared with M30, $$p < 0.001$ when compared with CORT + M30 groups,! $p < 0.001$ when compared with Vehicle.

doi:10.1371/journal.pone.0166966.g004

treated group when compared with those of the control or vehicle group ($p<0.001$ for synapsin-1, $p<0.01$ for synaptophysin and PSD-95) (n = 8, Fig 7). The decreased expressions were significantly mitigated by the M30 treatment (Fig 7).

M30 prevented CORT-induced neurodegeneration

The CORT-treated group had significant reductions in the density of dendritic spine, dendritic length, soma size and the volume of both basal and apical branches of CA1 and CA3 pyramidal neurons when compared to the control or vehicle group ($p<0.05$ for all) (n = 12, Fig 8). There were significant formations of varicosity on the CORT-treated apical and basal dendrites, which were indicated by the arrows in the Fig 8. However, these reductions and formation of varicosity were not observed in the group co-treated with M30 (Fig 8).

Discussion

It is the first report on the neuroprotective mechanism of M30 against depressive-like behavior resulting from altered serotonin metabolism and depletion of serotonin availability, loss of synaptic proteins and disrupted dendritic neuroarchitecture induced by chronic exposure to CORT. Importantly, we have demonstrated that M30 effectively prevented the pathophysiological consequence upon exaggerated MAO activation, namely oxidative stress and neuroinflammation, which significantly contributes to IDO-1 activation, serotonin deficiency and neurodegeneration. In fact, chronic CORT treatment induced significant depressive-like symptoms accompanied by serotonin deficiency and damaged neuronal structure in the hippocampus, the major brain region responsible for the negative feedback loop of hypercortisolemia. In our study, we have performed forced swimming test and reward-based sucrose preference test to assess behavioral despair and anhedonia, the main phenotypes of depression. Our results demonstrated that there were significant increases in immobility time and decreases in the percentage of sucrose consumption in the CORT-treated group (Fig 1 Panel A and B). These observations are in consistent with previous reports showing the depressive behavior induced by CORT treatment in the rat [5, 31]. In addition, it has been reported that a high dose (50 mg/kg) of CORT is required for the induction of depressive-like behaviors in a 2-week experimental paradigm [5]. This paradigm could consistently induce the pathophysiological cascade leading to neurodegeneration and also it could minimize the confounding side effects of CORT administration over months and the suffering of repeated CORT injections and the number of animals used for the study because of the increased variability and inconsistency of the end point measurements. Besides, the dose of M30 used in this study has been reportedly without adverse impacts on the physiological functions of healthy animals and no any toxicity effect was observed in animals given chronic treatment of M30 [22, 32, 33]. Particularly, M30 administration at the dose of 5mg/kg, which is reportedly the lowest dose effective for the neuroprotection, does not cause the most probable side effects of MAO inhibitors,

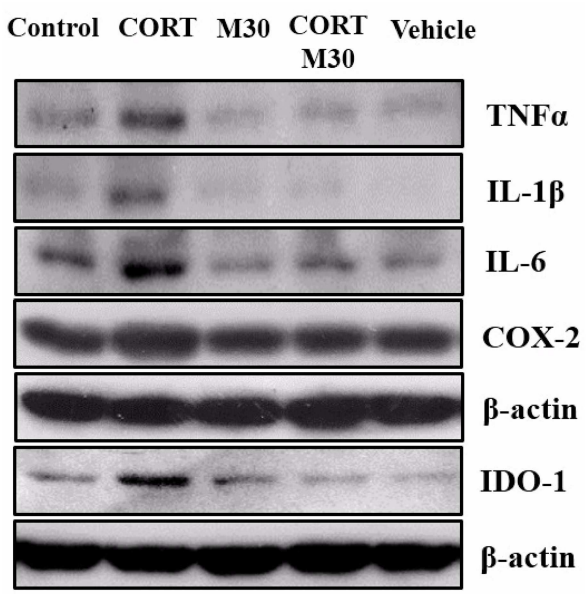
Control
CORT
M30
CORT M30
Vehicle
TNFα
IL-1β
IL-6
COX-2
β-actin
IDO-1
β-actin

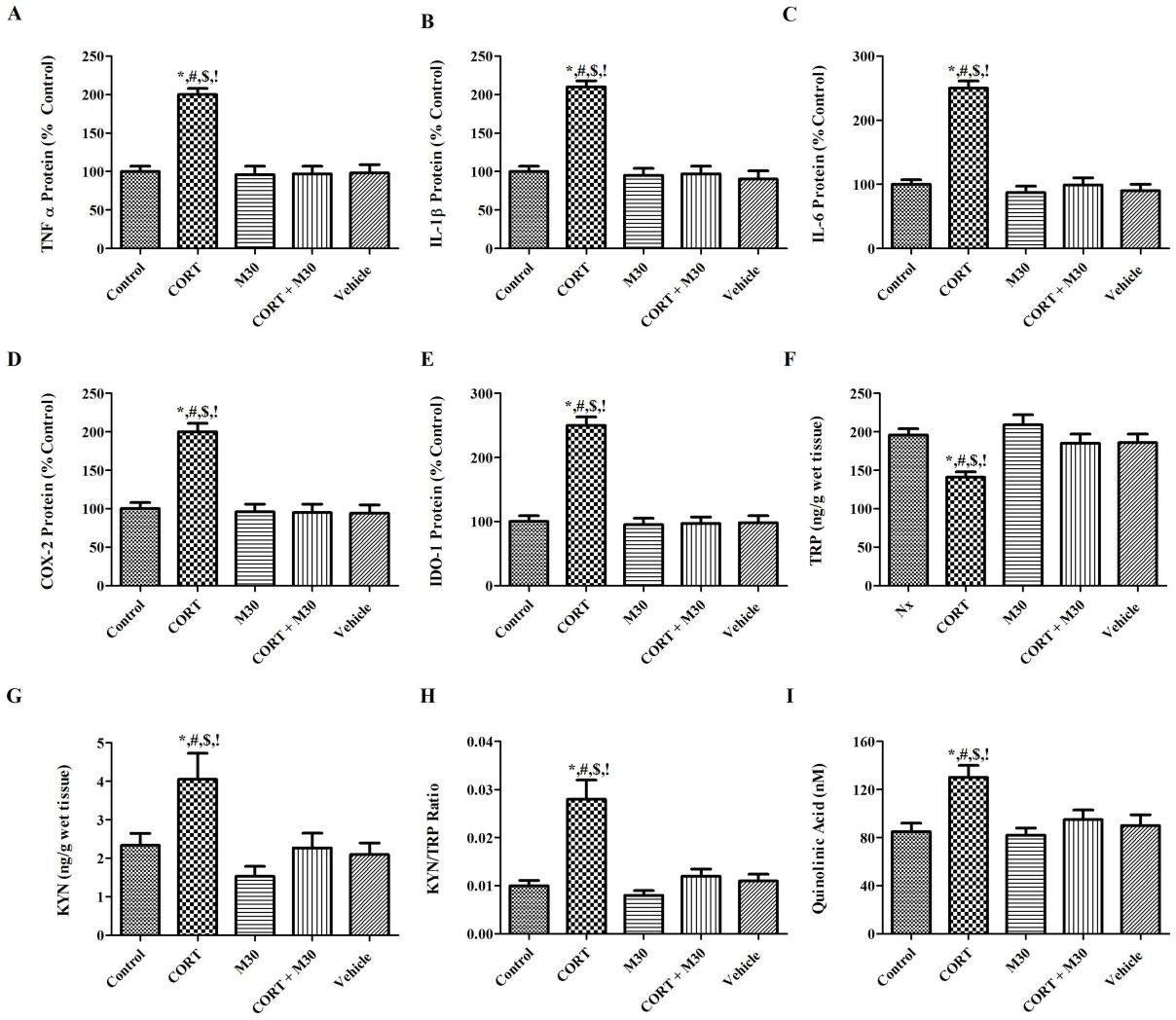
A
TNF α Protein (% Control)
B
IL-1β Protein (% Control)
C
IL-6 Protein (% Control)
D
COX-2 Protein (% Control)
E
IDO-1 Protein (% Control)
F
TRP (ng/g wet tissue)
G
KYN (ng/g wet tissue)
H
KYN/TRP Ratio
I
Quinolinic Acid (nM)
*,#,$,!
Control
CORT
M30
CORT + M30
Vehicle
Nx

Fig 5. Chronic CORT treatment induced neuroinflammation and activated cytokine-responsive IDO-1 in the rat hippocampus, which was significantly mitigated by M30 administration. Levels of the protein expression (A) TNFα, (B) IL-1β, (C) IL-6, (D) COX-2, (E) IDO-1, (F) TRP, (G) KNY, (H) the ratio of KYN/TRP (IDO-1 activity) and (I) the level of QUIN in the hippocampus of the control, CORT-treated (CORT), M30-treated (M30), CORT and M30 co-treated (CORT+M30) or vehicle groups are summarized. Data from each group were expressed as mean ± SEM (n = 8). Statistical comparisons between groups were performed using the One way Anova followed by Tukey post hoc test to detect differences in all groups. For TNFα, IL-1β, IL-6 and COX-2, *$p < 0.001$ when compared with Control, $^{\#}p < 0.001$ when compared with M30, $^{\$}p < 0.001$ when compared with CORT + M30 groups,$^{!}$ $p < 0.001$ when compared with Vehicle. For TRP, KYN, KYN/TRP and QUIN, *$p < 0.01$ when compared with Control, $^{\#}p < 0.01$ when compared with M30, $^{\$}p < 0.01$ when compared with CORT + M30 groups,$^{!}$ $p < 0.01$ when compared with Vehicle.

doi:10.1371/journal.pone.0166966.g005

namely the cheese effects, because M30 is a brain-selective MAO-inhibitor and poorly effects on small intestinal MAO-A activities [34].

We found that the antagonistic effect of M30 on the MAO activity is crucial to the protective action against CORT-induced depression. MAO-A plays a primary role in the maintenance of homeostatic levels of monoamines namely serotonin, norepinphrine and dopamine in the brain. Under pathophysiological conditions, persistent over-activation of the MAO-A activity could result in excessive turnover of monoamines leading to imbalance and deficiency, which significantly contributes to the induction of depressive symptoms. Indeed, we found that there was a significant increase in the MAO-A activity in the CORT-treated group, resulting in elevated serotonin catabolism and lowered serotonin levels in the hippocampus, which were markedly prevented by the co-treatment of M30. This finding is consistent with previous reports that abnormal activation of MAO-A and augmented serotonin turnover were present in the brain of depressed patients and stress-induced depression in animals, in which the depressive symptoms could be ameliorated by MAO-A inhibitors [35–37]. Intriguingly, no observable changes in the levels of 5-HT and 5-HIAA in the M30-treated group suggesting the activation of intrinsic cellular compensatory mechanism to prevent the accumulation of 5-HT leading to toxicity. In addition to be degraded by MAO-A, 5-HT can also be converted to N-acetyltransferase or so called arylalkylamine N-acetyltransferase (AANAT). AANAT has been demonstrated to present in the rat brain, particularly prominent in pineal gland, hippocampus, olfactory bulb, cerebellum, and spinal cord [38]. The levels of 5-HT and 5-HIAA depends on the balance between 5-HT accumulation due to MAO-A inhibition and activation of intrinsic cellular compensatory response

In addition to the deregulated serotonin turnover, over-activation of MAO-A induced by chronic CORT treatment disrupts redox balance as a result of the production of hydrogen peroxide as an enzymatic by-product of catalytic deamination of monoamines. This could significantly increase the production of reactive oxygen species (ROS) that oxidize the lipid membrane forming the MDA, and depleting endogenous antioxidant GSH capacity. In fact, our results showed that chronic CORT treatment significantly increased the MDA level accompanied by decreases in the GSH to GSSG ratio and the protein expression of antioxidant enzymes SOD-2 and GPx-1 in the hippocampus. Remarkably, these aberrant changes could be neutralized by the concurrent administration of M30, highlighting the antioxidant property of M30 against oxidative stress in addition to the MAO inhibition. These results are eventually in line with previous reports demonstrating M30 treatment can ameliorate oxidative stress in in-vivo studies by restoring antioxidant capacity and chelating excessive free radicals [39, 40].

We and others had shown that neuroinflammation was tightly associated with oxidative stress [26, 41]. Oxidative damage of the tissue could lead to the robust release of inflammatory

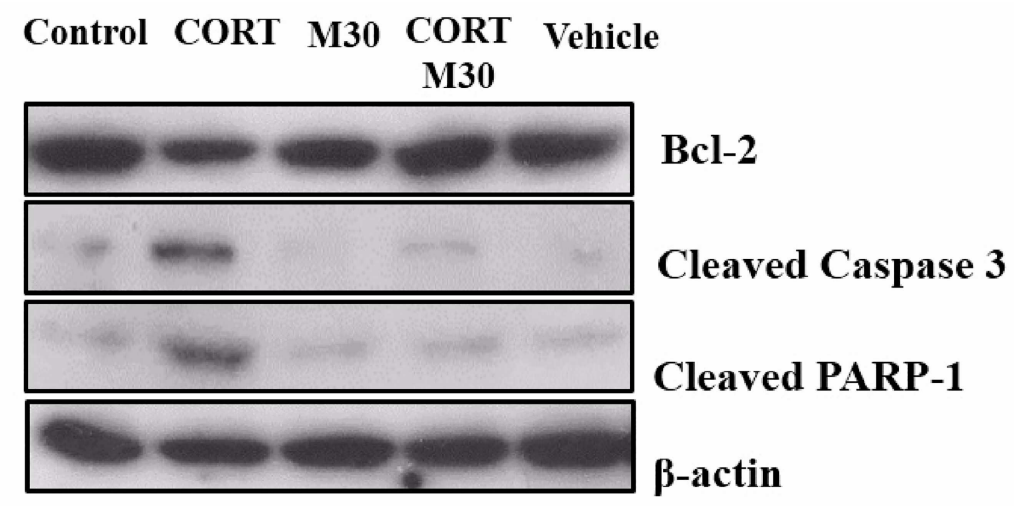
Control
CORT
M30
CORT M30
Vehicle
Bcl-2
Cleaved Caspase 3
Cleaved PARP-1
β-actin

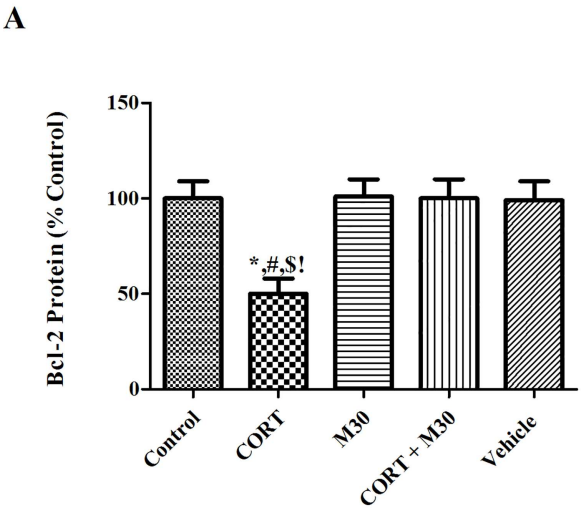
A
Bcl-2 Protein (% Control)
150
100
50
0
*,#,$!
Control
CORT
M30
CORT + M30
Vehicle

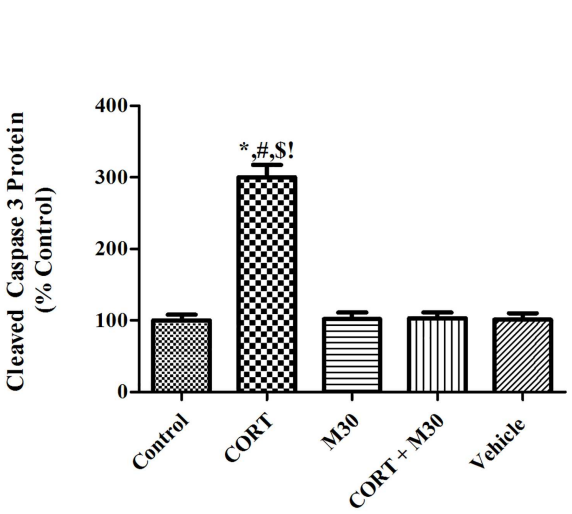
B
Cleaved Caspase 3 Protein (% Control)
400
300
200
100
0
*,#,$!
Control
CORT
M30
CORT + M30
Vehicle

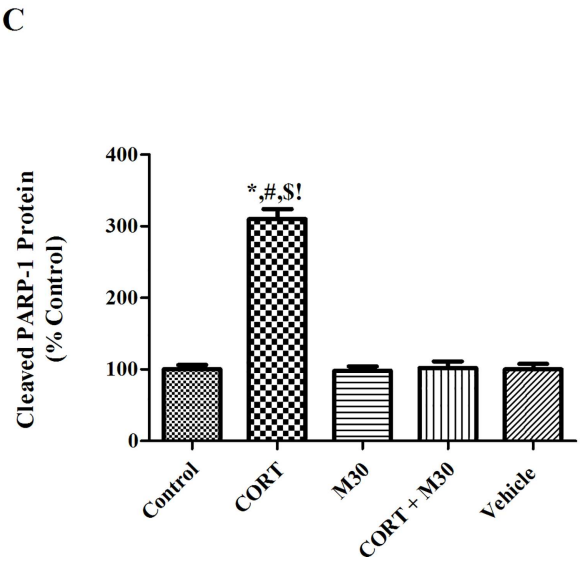
C
Cleaved PARP-1 Protein (% Control)
400
300
200
100
0
*,#,$!
Control
CORT
M30
CORT + M30
Vehicle

Fig 6. M30 abrogated CORT-induced hippocampal apoptosis. Levels of protein expression of (A) Bcl-2, (B) Cleaved Caspase 3 and (C) Cleaved PARP-1 in the hippocampus of the control, CORT-treated (CORT), M30-treated (M30), CORT and M30 co-treated (CORT+M30) or vehicle groups are summarized. β-actin was an internal control. Data from each group were expressed as mean ± SEM (n = 8). Statistical comparisons between groups were performed using the One way Anova followed by Tukey post hoc test to detect differences in all groups. For Bcl-2, *p < 0.01 when compared with Control, $^{\#}$p < 0.01 when compared with M30, $^{\$}$p < 0.01 when compared with CORT + M30 groups,$^{!}$ p < 0.01 when compared with Vehicle. For cleaved caspase 3 and cleaved PARP-1, *p < 0.001 when compared with Control, $^{\#}$p < 0.001 when compared with M30, $^{\$}$p < 0.001 when compared with CORT + M30 groups,$^{!}$ p < 0.001 when compared with Vehicle.

doi:10.1371/journal.pone.0166966.g006

cytokines through the activation of redox-sensitive NFκB canonical pathway. Additionally, these inflammatory mediators exacerbated the positive feedback loop among oxidative stress, inflammation and the tissue damages. Our results showed NFκB canonical pathway was activated through the degradation of the inhibitory protein IκBα leading to the translocation of NFκB members which induced their downstream inflammatory candidates such as TNF-α, IL-1β, IL-6 and COX-2 in the CORT-treated group, but these were potently repressed by M30 treatment. Overwhelming production of hydrogen peroxide is formed as a result of elevated MAO-A activities that serve as an important source of free radicals leading to the development vicious cycle of oxidative stress, neuroinflammation and cellular injuries. The anti-inflammatory ability of M30 demonstrated is possibly attributed to the blockade of vicious cycle through MAO-A inhibition as MAO-A is an early target gene upregulated by CORT and induce significant oxidative stress. In addition, the anti-inflammatory activity of M30 is also conferred by propargylamine moiety that is the same seen in rasagiline (Azilect) and Ladostigil which have been shown pronounced anti-inflammatory ability [42, 43]. Importantly, these inflammatory mediators triggered cytokine-sensitive IDO-1, the catabolic enzyme of serotonin and tryptophan which is the precursor of serotonin biosynthesis [44, 45]. The elevated IDO-1 activity could increase the conversion of tryptophan into kynurenine, which could decrease the tryptophan availability for serotonin synthesis resulting in serotonin deficiency. This is supported by our results showing significant increases in IDO-1 expression and activity along with a remarkable decrease in serotonin level in the hippocampus of CORT-treated group. These results are in agreement with the previous report which the activation of IDO-1 leading to serotonin deficiency involved in the progression of depressive-like behavior, which could be hindered by application of anti-inflammatory agent [46, 47]. Significantly, the administration of M30 mitigated the CORT-induced neuroinflammation, which is a result of the lowered MAO activity and oxidative stress targeted by M30. In addition to IDO-1, TDO-2 is another enzyme mediating tryptophan metabolism. However, TDO-2 is hardly detectable in the hippocampus of rat and responsive to elevated levels of inflammatory cytokines [48]. In our study, we have shown that there were significant elevations in the inflammatory cytokines which is pivotal to the activation of IDO-1 which subsequently reduced the level of 5-HT in the hippocampus. Our observation is in agreement with the previous reports demonstrating the activation of IDO-1 accompanied by the reduction in the 5-HT content in response to immune activation in the hippocampus of rat [49, 50]. Therefore, it should be IDO-1 instead of TDO-2 mediating the tryptophan breakdown in the hippocampus.

Apoptosis significantly contributes to neuroarchitectural changes that observed in clinically depressed patients and in animals [51, 52]. Our previous studies have shown that oxidative stress and inflammation could lead to neuronal apoptosis through the activation of intrinsic and extrinsic apoptotic cascades [26, 53]. Consistently, oxidative stress and inflammation induced by chronic CORT treatment trigger neuronal apoptosis evidenced by elevated levels of apoptotic markers cleaved caspase-3 and cleaved PARP-1 along with significant decreases in the anti-apoptotic protein Bcl-2. The apoptosis was significantly abrogated by M30

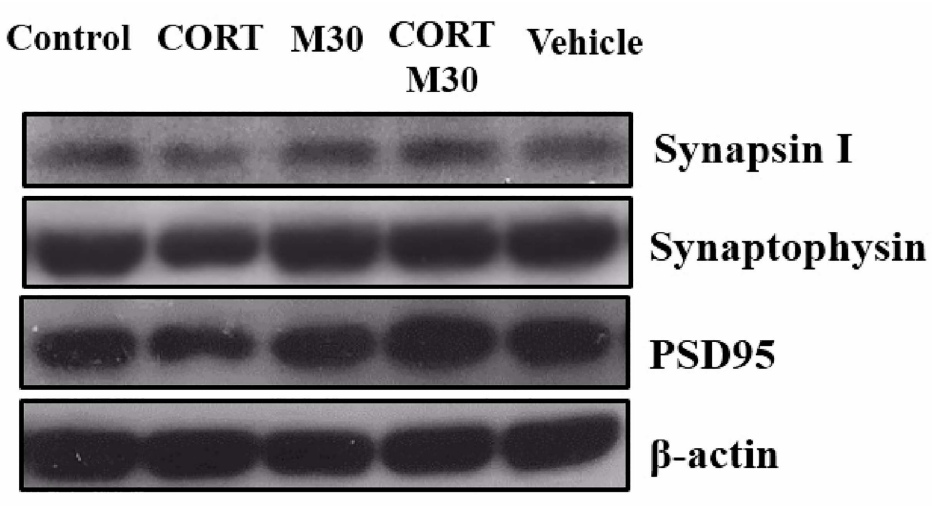
Control
CORT
M30
CORT M30
Vehicle
Synapsin I
Synaptophysin
PSD95
β-actin

A

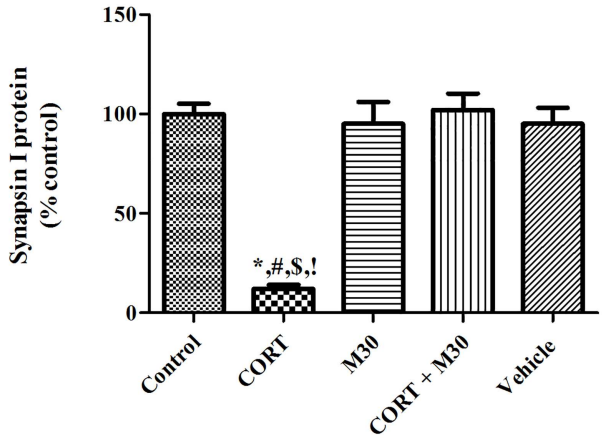
Synapsin I protein (% control)
150
100
50
0
*,#,$,!
Control
CORT
M30
CORT + M30
Vehicle

B

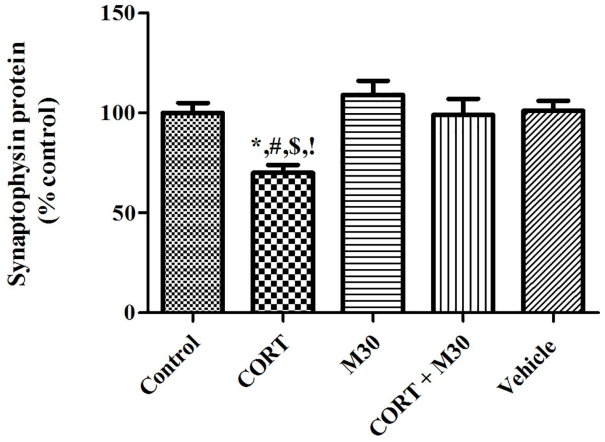
Synaptophysin protein (% control)
150
100
50
0
*,#,$,!
Control
CORT
M30
CORT + M30
Vehicle

C

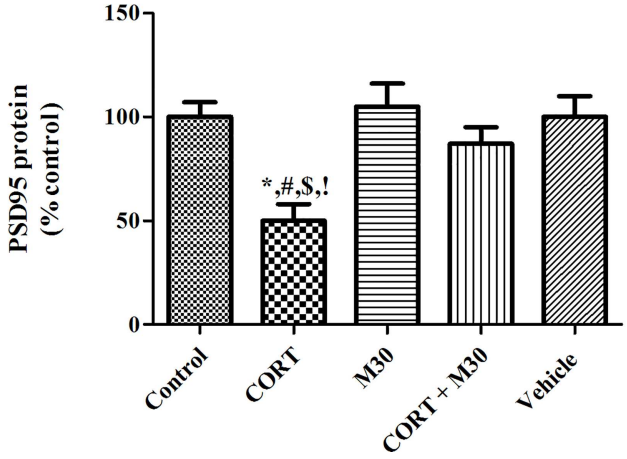
PSD95 protein (% control)
150
100
50
0
*,#,$,!
Control
CORT
M30
CORT + M30
Vehicle

Fig 7. Chronic CORT treatment induced loss of synaptic proteins in the hippocampus, which was significantly restored by M30 pre-treatment. Levels of protein expression of (A) Synapsin-1, (B) Synaptophysin and (C) PSD 95 in the hippocampus of the control, CORT-treated (CORT), M30-treated (M30), CORT and M30 co-treated (CORT+M30) or vehicle groups are summarized. β-actin was an internal control. For synapsin-1, *$p < 0.001$ when compared with Control, $^{\#}p < 0.001$ when compared with M30, $^{\$}p < 0.001$ when compared with CORT + M30 groups,$^{!}$ $p < 0.001$ when compared with Vehicle. For synaptophysin, *$p < 0.01$ when compared with Control, $^{\#}p < 0.001$ when compared with M30, $^{\$}p < 0.05$ when compared with CORT + M30 groups,$^{!}$ $p < 0.01$ when compared with Vehicle. For PSD-95, *$p < 0.01$ when compared with Control, $^{\#}p < 0.01$ when compared with M30, $^{\$}p < 0.05$ when compared with CORT + M30 groups,$^{!}$ $p < 0.01$ when compared with Vehicle.

doi:10.1371/journal.pone.0166966.g007

treatment, suggesting that blockade of MAO over-activity, oxidative stress and neuroinflammation are mechanistically involved in the anti-apoptotic effect of M30. Also, our results give support to previous findings showing anti-apoptotic effect of M30 in the brain of animals treated with dexamethasone or neurotoxin MPTP [22, 54].

Synaptic degeneration is suggested to be closely connected to the pathogenesis of depression, resulting from a significant loss of pre- and post-synaptic proteins [55, 56]. Pre-synaptic vesicle proteins play a role in the release of neurotransmitter into the synaptic cleft facilitating the neuronal communication while post-synaptic proteins orchestra the received pre-synaptic signal that in turn to adjust and fine-tune the activity of the dendritic spine [57, 58]. We found that chronic CORT treatment markedly down-regulated the pre-synaptic vesicle proteins synapsin-1 and synaptophysin and the post-synaptic protein PSD-95. These results are in agreement with previous reports showing that chronic CORT treatment could induce significant losses of synaptic proteins [5, 6], which are mediated by apoptotic caspase enzymes [59]. The fact that M30 significantly prevents the loss of synaptic proteins, strongly suggesting that a pathophysiological cascade mediated by MAO over-activity, oxidative stress, neuroinflammation and apoptosis, impeding the loss of synaptic proteins induced by CORT.

Moreover, we found that there were reduced dendritic length and spine density in both apical and basal branches of the CA3 and CA1 pyramidal neurons upon the CORT treatment. It was reported that NMDA excitotoxicity induced by CORT exposure causes the formation of varicosities in the dendritic spine and reduces the spine density [60]. In fact, quinolinic acid, an end product of breaking down tryptophan by IDO-1, is a ligand of NMDA receptors and possibly plays a role in the varicosity formation as a result of the elevated IDO-1 activity upon the CORT treatment [61]. This is supported by the fact that IDO-1 expression and activity, and the level of QUIN were significantly attenuated by the M30 treatment. Consequently, M30 could prevent the varicosity formation and preserve the reduced spine density induced by CORT. Our findings are in agreement with previous observations that impaired dendritic plasticity induced by chronic stress could be rescued by MAO inhibitor [62]. Furthermore, soma size and volume were decreased by the CORT treatment, which could be attributed to the pathogenic processes of neuronal apoptosis when DNA is fragmented and chromatin are condensed [63]. This could explain the protective effect of M30 treatment on the decreased soma size and volume shown in our results. Hence, multifunctional properties of M30 are important to prevent CORT-induced depression and the mechanistic effects of M30 against depressive-like behavior are summarized in the S2 Fig.

Conclusion

We have demonstrated the neuroprotective mechanism of selective brain MAO inhibitor M30 against CORT-induced depressive behavior by preventing altered serotonin metabolism mediated by elevated MAO-A and cytokine-sensitive IDO-1 activities, and by antagonizing the loss of synaptic protein and impaired dendritic morphologies mediated by oxidative stress, inflammation and apoptosis. Importantly, these works suggest that overactivities of MAO-A and

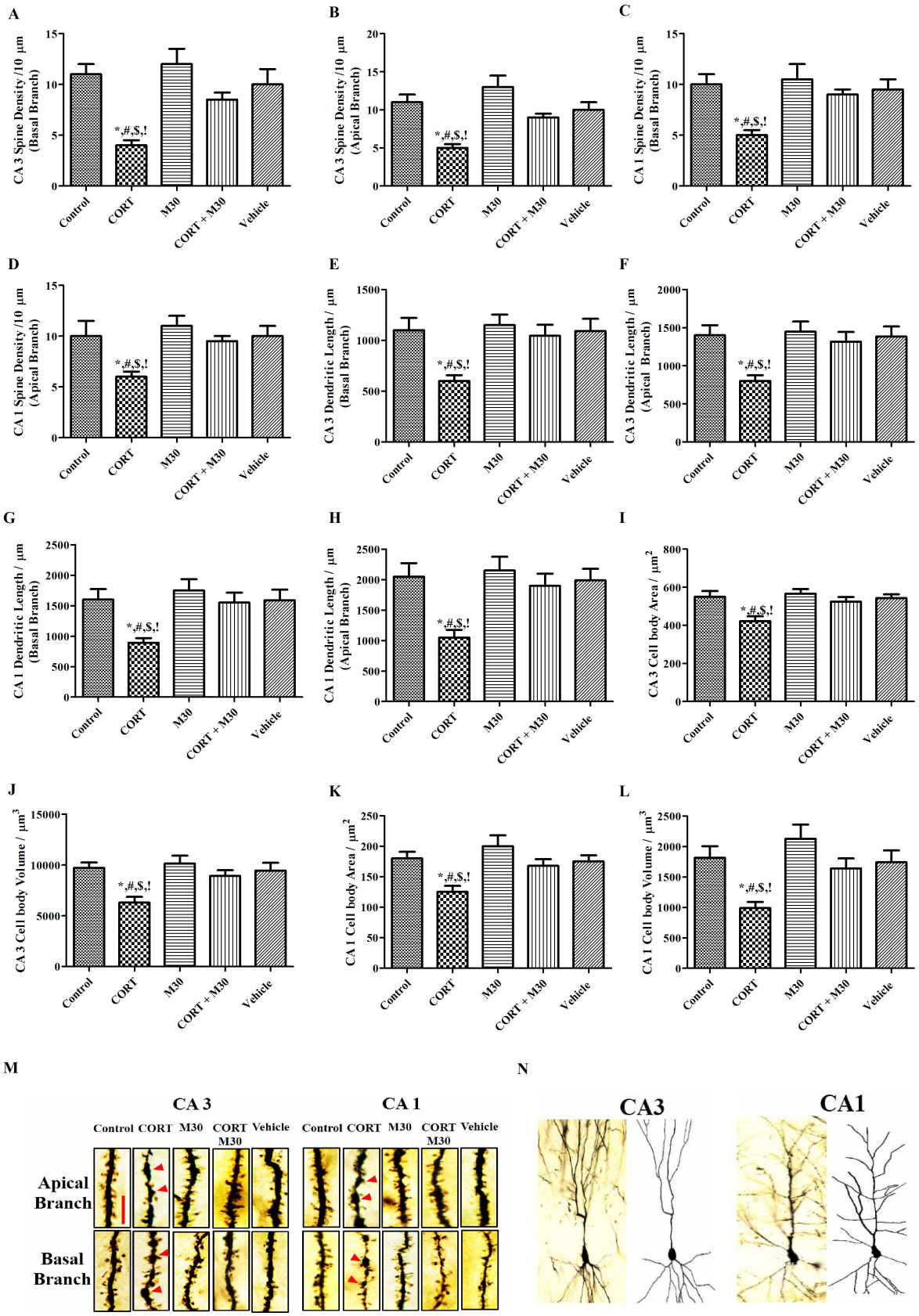
A
CA 3 Spine Density /10 μm (Basal Branch)
B
CA 3 Spine Density /10 μm (Apical Branch)
C
CA 1 Spine Density /10 μm (Basal Branch)
D
CA 1 Spine Density /10 μm (Apical Branch)
E
CA 3 Dendritic Length / μm (Basal Branch)
F
CA 3 Dendritic Length / μm (Apical Branch)
G
CA 1 Dendritic Length / μm (Basal Branch)
H
CA 1 Dendritic Length / μm (Apical Branch)
I
CA 3 Cell body Area / μm2
J
CA 3 Cell body Volume / μm3
K
CA 1 Cell body Area / μm2
L
CA 1 Cell body Volume / μm3
*,#,$,!
Control
CORT
M30
CORT + M30
Vehicle
M
CA 3
CA 1
Control CORT M30 CORT + M30 Vehicle
Apical Branch
Basal Branch
N
CA3
CA1

Fig 8. Chronic CORT treatment induced remarkable reductions in dendritic spine density, dendritic length, soma size and volume of both apical and basal branches of CA3 and CA1 pyramidal neurons. M30 administration prevented the aberrant morphological alteration. Dendritic varicosity formations responsible for reduction in dendritic spine density were indicated by the arrows. Dendritic spine densities of apical and basal CA3 and CA1 pyramidal neurons were respectively summarized in Panels A to D. Dendritic length of apical and basal CA3 and CA1 pyramidal neurons were respectively summarized in Panels E to H. Cell bodies' areas and volumes of apical and basal CA3 and CA1 pyramidal neurons were respectively summarized in Panels I to L. Panel M summarized representative photomicrographs of apical and basal dendrites of both CA3 and CA1 pyramidal neurons showing dendritic spines. Magnification:100X, Scale bar = 10μm. Panel N illustrated Camera Lucida drawing of representative CA3 and CA1 pyramidal neurons. Data from each group were expressed as mean ± SEM (n = 12). Statistical comparisons between groups were performed using the One way Anova followed by Tukey post hoc test to detect differences in all groups. *$p < 0.05$ when compared with Control, $^{\#}p < 0.05$ when compared with M30, $^{\$}p < 0.05$ when compared with CORT + M30 groups,$^{!}$ $p < 0.05$ when compared with Vehicle.

doi:10.1371/journal.pone.0166966.g008

IDO-1 play an important pathophysiological role in the CORT-induced depression, which can be effectively counteracted by M30.

Supporting Information

S1 Table. Chronic CORT treatment induced hypercortisolemia in the rats. Data from each group were expressed as mean ± SEM (n = 12). Statistical comparisons between groups were performed using the One way Anova followed by Tukey post hoc test to detect differences in all groups. $^{*}p < 0.001$ when compared with Control, $^{\#}p < 0.001$ when compared with Vehicle group.
(PDF)

S1 Fig. Chronic CORT treatment elevated protein expression levels of MAO-A and MAO-B, which were markedly attenuated by the M30 treatment. Protein expression levels of (A) MAO-A and (B) MAO-B in the hippocampus of the normoxic (Nx), CORT-treated (CORT), M30-treated (M30), CORT and M30 co-treated (CORT+M30) or vehicle groups are summarized in the figures. β-actin was an internal control. Data from each group were expressed as mean ± SEM (n = 8). Statistical comparisons between groups were performed using the One way Anova followed by Tukey post hoc test to detect differences in all groups. For MAO-A and MAO-B protein expressions, $^{*}p < 0.001$ when compared with Control, $^{\#}p < 0.001$ when compared with M30, $^{\$}p < 0.001$ when compared with Vehicle groups,$^{!}$ $p < 0.001$ when compared with Control, $^{\wedge}p < 0.001$ when compared with M30, $^{\%}p < 0.001$ when compared with Vehicle groups. For MAO-B activity, $^{*}p < 0.001$ when compared with Control, $^{\#}p < 0.001$ when compared with M30, $^{\$}p < 0.001$ when compared with CORT + M30 groups,$^{!}$ $p < 0.001$ when compared with Vehicle, $^{\wedge}p < 0.001$ when compared with Control, $^{\%}p < 0.001$ when compared with CORT + M30, $^{\&}p < 0.001$ when compared with Vehicle groups
(PDF)

S2 Fig. Schematic diagram illustrates the neuroprotective mechanism of M30 against depressive like behavior induced by CORT.
(PDF)

Acknowledgments

We are grateful for the technical support of Mr. Y.M. Lo.

Author Contributions

Conceptualization: MLF GLT CSL.

Data curation: MLF GLT CSL.

Formal analysis: CSL.

Funding acquisition: MLF.

Investigation: MLF GLT CSL.

Methodology: MLF GLT CSL.

Project administration: MLF.

Resources: MLF GLT JKCW MBHY.

Software: MLF GLT.

Supervision: MLF GLT.

Validation: MLF GLT CSL.

Visualization: MLF GLT CSL.

Writing – original draft: CSL.

Writing – review & editing: MLF.

References

1. Bromet E, Andrade LH, Hwang I, Sampson NA, Alonso J, De Girolamo G, et al., Cross-national epidemiology of DSM-IV major depressive episode. BMC Medicine. 2011; 9(1): p. 90.
2. Kessler RC, Berglund P, Demler O, Jin R, Koretz D, Merikangas KR, et al., The epidemiology of major depressive disorder: results from the National Comorbidity Survey Replication (NCS-R). JAMA. 2003; 289(23): p. 3095–3105. doi: 10.1001/jama.289.23.3095 PMID: 12813115
3. Carroll B, Iranmanesh A, Keenan DM, Cassidy F, Wilson WH, Veldhuis JD. Pathophysiology of hypercortisolism in depression: pituitary and adrenal responses to low glucocorticoid feedback. Acta Psychiatrica Scandinavica. 2012; 125(6): p. 478–491. doi: 10.1111/j.1600-0447.2011.01821.x PMID: 22211368
4. Sheline YI, Wang PW, Gado MH, Csernansky JG, Vannier MW. Hippocampal atrophy in recurrent major depression. Proceedings of the National Academy of Sciences. 1996; 93(9): p. 3908–3913.
5. Yau SY, Li A, Zhang ED, Christie BR, Xu A, Lee T, et al. Sustained running in rats administered corticosterone prevents the development of depressive behaviors and enhances hippocampal neurogenesis and synaptic plasticity without increasing neurotrophic factor levels. Cell Transplantation. 2014; 23(4–5): p. 481–492. doi: 10.3727/096368914X678490 PMID: 24816445
6. Zhang ESY, Lau BWM, Ma H, Lee T, Chang RCC, et al. Synaptic Plasticity, But Not Hippocampal Neurogenesis, Mediated the Counteractive Effect of Wolfberry on Depression in Rats1. Cell Transplantation. 2012; 21(12): p. 2635–2649. doi: 10.3727/096368912X655181 PMID: 23127884
7. Youdim MB, Riederer PF. A review of the mechanisms and role of monoamine oxidase inhibitors in Parkinson's disease. Neurology. 2004; 63(7 suppl 2): p. S32–S35.
8. Youdim MB, Bakhle Y. Monoamine oxidase: isoforms and inhibitors in Parkinson's disease and depressive illness. British Journal of Pharmacology. 2006; 147(S1): p. S287–S296.
9. Du L, Bakish D, Ravindran A, Hrdina PD. MAO-A gene polymorphisms are associated with major depression and sleep disturbance in males. Neuroreport. 2004; 15(13): p. 2097–2101. PMID: 15486489
10. Du L, Faludi G, Palkovits M, Sotonyi P, Bakish D, Hrdina PD. High activity-related allele of MAO-A gene associated with depressed suicide in males. Neuroreport. 2002; 13(9): p. 1195–1198. PMID: 12151768
11. Meyer JH, Wilson AA, Sagrati S, Miler L, Rusjan P, Bloomfield PM, et al. Brain monoamine oxidase A binding in major depressive disorder: relationship to selective serotonin reuptake inhibitor treatment, recovery, and recurrence. Archives of General Psychiatry. 2009; 66(12): p. 1304–1312. doi: 10.1001/archgenpsychiatry.2009.156 PMID: 19996035
12. Grunewald M, Johnson S, Lu D, Wang Z, Lomberk G, Albert PR, et al. Mechanistic role for a novel glucocorticoid-KLF11 (TIEG2) protein pathway in stress-induced monoamine oxidase A expression.

Journal of Biological Chemistry. 2012; 287(29): p. 24195–24206. doi: 10.1074/jbc.M112.373936 PMID: 22628545

13. Lee HY, Lee GH, Marahatta A, Lin SM, Lee MR, Jang KY, et al. The protective role of Bax Inhibitor-1 against chronic mild stress through the inhibition of monoamine oxidase A. Scientific Reports. 2013; 3; doi: 10.1038/srep03398 PMID: 24292328
14. Barton DA, Esler MD, Dawood T, Lambert EA, Haikerwal D, Brenchley C, et al. Elevated brain serotonin turnover in patients with depression: effect of genotype and therapy. Archives ofGeneral Psychiatry. 2008; 65(1): p. 38–46.
15. Dale E, Bang-Andersen B, Sánchez C. Emerging mechanisms and treatments for depression beyond SSRIs and SNRIs. Biochemical pharmacology 95(2): p. 81–97 (2015). doi: 10.1016/j.bcp.2015.03.011 PMID: 25813654
16. Setiawan E, Bang-Andersen B, Sánchez C. Role of translocator protein density, a marker of neuroinflammation, in the brain during major depressive episodes. JAMA Psychiatry. 2015; 72(3): p. 268–275. doi: 10.1001/jamapsychiatry.2014.2427 PMID: 25629589
17. Liu YN, Peng YL, Wu TY, Zhang Y, Lian YJ, Yang YY, et al. TNFα mediates stress-induced depression by upregulating indoleamine 2, 3-dioxygenase in a mouse model of unpredictable chronic mild stress. European Cytokine Network. 2015; 26(1): p. 15–25. doi: 10.1684/ecn.2015.0362 PMID: 26083579
18. O'connor J, Lawson M, Andre C, Moreau M, Lestage J, Castanon N, et al. Lipopolysaccharide-induced depressive-like behavior is mediated by indoleamine 2, 3-dioxygenase activation in mice. Molecular Psychiatry. 2009; 14(5): p. 511–522. doi: 10.1038/sj.mp.4002148 PMID: 18195714
19. Okuda S, Nishiyama N, Saito H, Katsuki H. 3-Hydroxykynurenine, an endogenous oxidative stress generator, causes neuronal cell death with apoptotic features and region selectivity. Journal of Neurochemistry. 1998; 70(1): p. 299–307. PMID: 9422375
20. Schurr A, West CA, Rigor B. Neurotoxicity of quinolinic acid and its derivatives in hypoxic rat hippocampal slices. Brain Research. 1991; 568(1): p. 199–204.
21. Youdim MB. Multi target neuroprotective and neurorestorative anti-Parkinson and anti-Alzheimer drugs ladostigil and m30 derived from rasagiline. Experimental Neurobiology. 2013; 22(1): p. 1–10. doi: 10.5607/en.2013.22.1.1 PMID: 23585716
22. Gal S, Zheng H, Fridkin M, Youdim MB. Novel multifunctional neuroprotective iron chelator-monoamine oxidase inhibitor drugs for neurodegenerative diseases. In vivo selective brain monoamine oxidase inhibition and prevention of MPTP-induced striatal dopamine depletion. Journal of Neurochemistry. 2005; 95(1): p. 79–88. doi: 10.1111/j.1471-4159.2005.03341.x PMID: 16181414
23. Weinreb O, Amit T, Bar-Am O, Youdim MB. Neuroprotective effects of multifaceted hybrid agents targeting MAO, cholinesterase, iron and β-amyloid in aging and Alzheimer's disease. British Journal of Pharmacology. 2016; 173(13):2080–94. doi: 10.1111/bph.13318 PMID: 26332830
24. Pimentel LS, Allard S, Do Carmo S, Weinreb O, Danik M, Hanzel CE, et al. The Multi-Target Drug M30 Shows Pro-Cognitive and Anti-Inflammatory Effects in a Rat Model of Alzheimer's Disease. Journal of Alzheimer's Disease2015; 47(2):373–83. doi: 10.3233/JAD-143126 PMID: 26401560
25. Hellsten J, WennstroÈm M, Mohapel P, Ekdahl CT, Bengzon J, TingstroÈm. Electroconvulsive seizures increase hippocampal neurogenesis after chronic corticosterone treatment. European Journal of Neuroscience. 2002; 16(2): p. 283–290. PMID: 12169110
26. Lam CS, Tipoe GL, So KF, Fung ML. Neuroprotective Mechanism of Lycium barbarum Polysaccharides against Hippocampal-Dependent Spatial Memory Deficits in a Rat Model of Obstructive Sleep Apnea. PLoS One 10(2): e0117990 (2015). doi: 10.1371/journal.pone.0117990 PMID: 25714473
27. Castagné V, Moser P, Roux S, Porsolt RD. Rodent models of depression: forced swim and tail suspension behavioral despair tests in rats and mice. Current Protocols in Neuroscience. 2011; 55(8.10): p. 11–18.10.
28. Slattery DA, Cryan JF. Using the rat forced swim test to assess antidepressant-like activity in rodents. Nature Protocols. 2012; 7(6): p. 1009–1014. doi: 10.1038/nprot.2012.044 PMID: 22555240
29. Strekalova T, Spanagel R, Bartsch D, Henn FA, Gass P. Stress-induced anhedonia in mice is associated with deficits in forced swimming and exploration. Neuropsychopharmacology. 2004; 29(11): p. 2007–2017. doi: 10.1038/sj.npp.1300532 PMID: 15266352
30. Willner P, Towell A, Sampson D, Sophokleous S, Muscat R. Reduction of sucrose preference by chronic unpredictable mild stress, and its restoration by a tricyclic antidepressant. Psychopharmacology. 1987; 93(3): p. 358–364. PMID: 3124165
31. Johnson SA, Fournier NM, Kalynchuk LE. Effect of different doses of corticosterone on depression-like behavior and HPA axis responses to a novel stressor. Behavioural Brain Research. 2006; 168(2): p. 280–288. doi: 10.1016/j.bbr.2005.11.019 PMID: 16386319

32. Bar-Am O, Amit T, Kupershmidt L, Aluf Y, Mechlovich D, Kabha H, et al. Neuroprotective and neurorestorative activities of a novel iron chelator-brain selective monoamine oxidase-A/monoamine oxidase-B inhibitor in animal models of Parkinson's disease and aging. Neurobiology of Aging. 2015; 36(3): p. 1529–1542. doi: 10.1016/j.neurobiolaging.2014.10.026 PMID: 25499799

33. Kupershmidt L, Amit T, Bar-Am O, Youdim MB, Weinreb O. The novel multi-target iron chelating-radical scavenging compound M30 possesses beneficial effects on major hallmarks of Alzheimer's disease. Antioxidants & Redox Signaling. 2012; 17(6): p. 860–877.

34. Gal S, Abassi ZA, Youdim MB. Limited potentiation of blood pressure in response to oral tyramine by the anti-Parkinson brain selective multifunctional monoamine oxidase-AB inhibitor, M30. Neurotoxicity Research. 2010; 18(2): p. 143–150. doi: 10.1007/s12640-009-9128-8 PMID: 19894083

35. Dhingra D, Bhankher A. Behavioral and biochemical evidences for antidepressant-like activity of palmatine in mice subjected to chronic unpredictable mild stress. Pharmacological Reports. 2014; 66(1): p. 1–9. doi: 10.1016/j.pharep.2013.06.001 PMID: 24905299

36. Liao JC, Tsai JC, Liu CY, Huang HC, Wu LY, Peng WH. Antidepressant-like activity of turmerone in behavioral despair tests in mice. BMC Complementary and Alternative Medicine. 2013; 13(1): p. 299.

37. Poltyrev T, Gorodetsky E, Bejar C, Schorer-Apelbaum D, Weinstock M. Effect of chronic treatment with ladostigil (TV-3326) on anxiogenic and depressive-like behaviour and on activity of the hypothalamic–pituitary–adrenal axis in male and female prenatally stressed rats. Psychopharmacology. 2005; 181(1): p. 118–125. doi: 10.1007/s00213-005-2229-z PMID: 15830235

38. Uz T, Sugaya K, Manev H. Neuronal expression of arylalkylamine N-acetyltransferase (AANAT) mRNA in the rat brain. Neuroscience Research. 2002; 42(4): p. 309–316. PMID: 11985883

39. Mechlovich D, Amit T, Mandel SA, Bar-Am O, Bloch K, Vardi P, Youdim MB. The novel multifunctional, iron-chelating drugs M30 and HLA20 protect pancreatic β-cell lines from oxidative stress damage. Journal of Pharmacology and Experimental Therapeutics. 2010; 333(3): p. 874–882. doi: 10.1124/jpet.109.164269 PMID: 20237072

40. Xiao J, Lv Y, Lin B, Tipoe GL, Youdim MB, Xing F, Liu Y. Novel Antioxidant Multitarget Iron Chelator M30 Protects Hepatocytes against Ethanol-Induced Injury. Oxidative Medicine and Cellular Longevity. 2015;607271; doi: 10.1155/2015/607271 PMID: 25722794

41. Kratsovnik E, Bromberg Y, Sperling O, Zoref-Shani E. Oxidative stress activates transcription factor NF-κB-mediated protective signaling in primary rat neuronal cultures. Journal ofMolecular Neuroscience. 2005; 26(1): p. 27–32.

42. Panarsky R, Luques L, Weinstock M. Anti-inflammatory effects of ladostigil and its metabolites in aged rat brain and in microglial cells. Journal of Neuroimmune Pharmacology. 2012; 7(2): p. 488–498. doi: 10.1007/s11481-012-9358-z PMID: 22454040

43. Trudler D, Weinreb O, Mandel SA, Youdim MB, Frenkel D. DJ-1 deficiency triggers microglia sensitivity to dopamine toward a pro-inflammatory phenotype that is attenuated by rasagiline. Journal of Neurochemistry. 2014; 129(3): p. 434–447. doi: 10.1111/jnc.12633 PMID: 24355073

44. Corona AW, Huang Y, O'Connor JC, Dantzer R, Kelley KW, Popovich PG, et al. Fractalkine receptor (CX3CR1) deficiency sensitizes mice to the behavioral changes induced by lipopolysaccharide. Journal of Neuroinflammation. 2010; 7(93.10): p. 1186.

45. Wichers MC, Maes M. The role of indoleamine 2, 3-dioxygenase (IDO) in the pathophysiology of interferon-α-induced depression. Journal of Psychiatry and Neuroscience. 2004; 29(1): p. 11. PMID: 14719046

46. Kim H, Chen L, Lim G, Sung B, Wang S, McCabe MF, et al. Brain indoleamine 2, 3-dioxygenase contributes to the comorbidity of pain and depression. The Journal of Clinical Investigation. 2012; 122(8): p. 2940. doi: 10.1172/JCI61884 PMID: 22751107

47. Xie W, Cai L, Yu Y, Gao L, Xiao L, He Q, et al., Activation of brain indoleamine 2, 3-dioxygenase contributes to epilepsy-associated depressive-like behavior in rats with chronic temporal lobe epilepsy. Journal of Neuroinflammation. 2014; 11: p. 41. doi: 10.1186/1742-2094-11-41 PMID: 24594021

48. Haber R, Bessette D, Hulihan-Giblin B, Durcan MJ, Goldman D. Identification of Tryptophan 2, 3-Dioxygenase RNA in Rodent Brain. Journal of Neurochemistry. 1993; 60(3): p. 1159–1162. PMID: 7679723

49. Chen WZ, Liu S, Chen FF, Zhou CJ, Yu J, Zhuang CL, et al., Prevention of Postoperative Fatigue Syndrome in Rat Model by Ginsenoside Rb1 via Down-Regulation of Inflammation along the NMDA Receptor Pathway in the Hippocampus. Biological and Pharmaceutical Bulletin. 2015; 38(2): p. 239–247. doi: 10.1248/bpb.b14-00599 PMID: 25747983

50. Xu Y, Sheng H, Tang Z, Lu J. Inflammation and increased IDO in hippocampus contribute to depression-like behavior induced by estrogen deficiency. Behavioural Brain Research. 2015; 288: p. 71–78. doi: 10.1016/j.bbr.2015.04.017 PMID: 25907742

51. Lucassen PJ, Fuchs E, Czéh B. Antidepressant treatment with tianeptine reduces apoptosis in the hippocampal dentate gyrus and temporal cortex. Biological Psychiatry. 2004; 55(8): p. 789–796. doi: 10.1016/j.biopsych.2003.12.014 PMID: 15050859

52. Malykhin NV, Carter R, Seres P, Coupland NJ. Structural changes in the hippocampus in major depressive disorder: contributions of disease and treatment. Journal of Psychiatry & Neuroscience. 2010; 35 (5): p. 337.

53. Hung MW, Tipoe GL, Poon AMS, Reiter RJ, Fung ML. Protective effect of melatonin against hippocampal injury of rats with intermittent hypoxia. Journal of Pineal Research. 2008; 44(2): p. 214–221. doi: 10.1111/j.1600-079X.2007.00514.x PMID: 18289174

54. Johnson S, Tazik S, Lu D, Johnson C, Youdim MB, Wang J. The new inhibitor of monoamine oxidase, M30, has a neuroprotective effect against dexamethasone-induced brain cell apoptosis. Frontiers in Neuroscience. 2010; 4:180; doi: 10.3389/fnins.2010.00180 PMID: 21103012

55. Marttinen M, Kurkinen KM, Soininen H, Haapasalo A, Hiltunen M. Synaptic dysfunction and septin protein family members in neurodegenerative diseases. Molecular Neurodegeneration. 2015; 10(1): p. 16.

56. Wuwongse S, Cheng SSY, Wong GTH, Hung CHL, Zhang NQ, Ho YS, et al. Effects of corticosterone and amyloid-beta on proteins essential for synaptic function: Implications for depression and Alzheimer's disease. Biochimica et Biophysica Acta (BBA)-Molecular Basis of Disease. 2013; 1832(12): p. 2245–2256.

57. Dosemeci A, Makusky AJ, Jankowska-Stephens E, Yang X, Slotta DJ, Markey SP. Composition of the synaptic PSD-95 complex. Molecular & Cellular Proteomics. 2007; 6(10): p. 1749–1760.

58. Rizzoli SO. Synaptic vesicle recycling: steps and principles. The EMBO Journal. 2014;p. e201386357 (2014).

59. Liu J, Chang L, Roselli F, Almeida O, Gao X, Wang X, et al. Amyloid-β induces caspase-dependent loss of PSD-95 and synaptophysin through NMDA receptors. Journal of Alzheimer's Disease 2009; 22(2): p. 541–556.

60. Hasbani MJ, Schlief ML, Fisher DA, Goldberg MP. Dendritic spines lost during glutamate receptor activation reemerge at original sites of synaptic contact. The Journal of Neuroscience. 2011; 21(7): p. 2393–2403.

61. Steiner J, Walter M, Gos T, Guillemin GJ, Bernstein H-G, Sarnyai Z, et al. Severe depression is associated with increased microglial quinolinic acid in subregions of the anterior cingulate gyrus: evidence for an immune-modulated glutamatergic neurotransmission. Journal of Neuroinflammation. 2011; 8(94): p. 1–9.

62. Morais M, Santos PA, Mateus-Pinheiro A, Patrício P, Pinto L, Sousa N, et al. The effects of chronic stress on hippocampal adult neurogenesis and dendritic plasticity are reversed by selective MAO-A inhibition. Journal of Psychopharmacology. 2014; 28(12): p. 1178–1183. doi: 10.1177/0269881114553646 PMID: 25315831

63. Elmore S. Apoptosis: a review of programmed cell death. Toxicologic Pathology. 2007; 35(4): p. 495–516. doi: 10.1080/01926230701320337 PMID: 17562483